IEEE Robotics and Automation Letters (RA-L) paper, presented at ICRA 2023, London, UK. Cite as RA-L paper.

Research on Target Tracking for Robotic Fish Based on Low-cost Scarce Sensing Information Fusion

Yong Zhong, *member, IEEE*, Youdong Chen, Chengcai Wang, Qixing Wang, and Jiawei Yang

***Abstract*—Target tracking for underwater robots is always challenging, due to low-quality sensing information, information interference, and environmental disturbances. Traditional sensing methods for underwater target tracking include vision-based tracking, acoustic-based tracking, etc., but most of the adopted sensors are extremely expensive or complicated to achieve the mission. In this paper, we investigate the possibility of utilizing low-cost scarce sensing information for underwater target tracking through a robotic fish platform. First, we introduce the design and control system of the robotic fish platform. Instead of using cameras and other expensive sensors, we adopt low-cost infrared sensors as the primary sensors for the robotic fish, which can only detect the appearance of objects within the sensing range of each sensor. Second, we present a target tracking strategy based on the scarce sensing information and fusion by analyzing and combining the information of two adjacent consecutive moments of the sensors. Then, a centralized detection decision tree with fewer branches, fast convergence, and high purity is proposed. Finally, to verify our method, several sets of guided target tracking experiments are conducted. The experimental results show the effectiveness and robustness of the proposed target tracking strategy based on low-cost scarce sensing information fusion.**

***Index Terms*—Robotic fish, sensor information fusion, centralized detection, decision tree, target tracking.**

I. Introduction

SINCE underwater vehicles can replace humans to explore the inaccessible and unpredictable marine environment, the exploration and cognition of the ocean have entered a stage of rapid development. As a new type of underwater vehicle, robotic fish has attracted the interests of scientists and engineers around the world. The world's first robotic fish, Robo Tuna [1], was successfully designed and developed by MIT in 1994. Subsequently, many different types of robotic fishes have been developed [2], such as 3D swimming robotic fish [3], robotic manta ray [4], boxfish-like robot [5, 6], amphibious robotic fish [7], soft robotic fish [8], wire-driven robotic fish of our team [9-11], and so on. Although there is a variety of robotic fishes, the capability of environmental perception still has a large gap with the real fish, such as target or predator perception, flow sensing, and acoustic sensing or communication. Moreover, most of the sensors available on land are not suitable for underwater environment.

To achieve the abovementioned similar functionalities of real fish, cameras, inertia measurement unit (IMU), pressure sensors, acoustic-based sensors, infrared sensors, and etc., are normally used to improve the perception capabilities for robotic fishes. Camera is one of the most widely used sensors to get visual information around[12, 13], but the availability of the information depends on the imaging quality of the camera. Some underwater robots employed acoustic-based GPS and sonar systems underwater localization and environment perception [14-16], but these sensors are extremely expensive and more suitable for use in vast waters. Some researchers mimic the function of lateral line of fish to sense water flow by installing multiple pressure sensors on the side of the robotic fish, i.e. the artificial lateral line system of robotic fish [17-19]. For the type of sensors that can only detect the appearance of an object (such as infrared sensors, ultrasonic transducers, etc.), they are mainly used for simple tasks such as obstacle avoidance, and when combined with IMU, direction tracking with obstacle avoidance can be achieved [20]. In summary, fully environmental perception like a real fish is still a great challenge for robotic fishes. Therefore, researchers usually only select sensors that meet their needs for research purposes, such as infrared sensors for obstacle avoidance, vision for target tracking, pressure sensors for flow sensing, and so on.

Target tracking, one of the basic underwater perceptional functions, has been a problematic and hot spot in the research of biomimetic robotic fish. Most of the target tracking of robotic fishes are based on visual information [12, 21]. In 2009, Xie et al developed a vision-based autonomous robotic fish and achieved underwater moving target tracking through a modified continuously adaptive mean shift (Camshift)

Manuscript received: November, 12, 2021; Revised January, 8, 2022; Accepted March, 14, 2022. This letter was recommended for publication by Editor Xinyu Liu upon evaluation of the reviewers' comments. This work was supported in part by the National Natural Science Foundation of China under Grant 62103152, the Natural Science Foundation of Guangdong Province (Grant No. 2020A1515010621), Guangzhou Applied Basic Research Foundation (202102020360), KEY Laboratory of Robotics and Intelligent Equipment of Guangdong Regular Institutions of Higher Education (Grant No.2017KSYS009), and Innovation Center of Robotics and Intelligent Equipment). (*Corresponding author: Chengcai Wang*)

Yong Zhong, Youdong Chen, Qixing Wang, and Jiawei Yang are with Shien-Ming Wu School of Intelligent Engineering, South China University of Technology, Guangzhou, China (email: zhongyong@scut.edu.cn; { 201920154516, 202121060425 201920154550} @mail.scut.edu.cn)

Chengcai Wang is with CETC Ocean Information Co., Ltd, Beijing, China (email: ccwang@pku.edu.cn)

algorithm. Yu et al. also adopted the Camshift algorithm to realize the tracking of the stationary target on a two-dimensional plane by processing the color information in robotic fish vision [22]. Based on the above, their team proposed a depth control method based on fuzzy sliding mode control to realize the tracking of robotic fish on a three-dimensional plane [23]. Camshift algorithm for target tracking is mainly based on the color information of the target. Still, when the target is close to the background color or is occluded by other objects, the Camshift algorithm will automatically include it, causing the tracking window to expand, resulting in inaccurate target positioning, and ultimately loss of the target. Another tracking method is to adopt global vision [24, 25]. Instead of installing a camera on the robotic fish, the camera is installed upright above the experimental pool. Although the centralized method of the global vision platform can produce the best-coordinated control, it is slow to respond to external changes, and it is impossible to obtain global visual information in truly open ocean waters. Moreover, due to the rich information from camera, the MCU on robotic fish platform needs time to process, which may cause slow response. In this work, we want to try the possibility to achieve the target tracking of robotic fish by only replying on scarce sensing information, not visual information.

We explore the feasibility of utilizing much simpler and cheaper sensors for target tracking tasks, such as infrared sensors, laser sensors, and ultrasonic transducers. Considering the size of the robotic fish, here, we adopt low-cost infrared sensors as the primary sensors as an example to achieve our mission. The infrared sensors can only detect the appearance of an object within the sensing range. In general, this scarce sensing information of infrared sensors is hard to deal with underwater target tracking. But we proposed a target tracking strategy based on the scarce sensing information and fusion through analyzing and combining the information of two adjacent consecutive moments of the sensors; and presented a centralized detection decision tree with fewer branches, fast convergence, and high purity for the motion decision of the robotic fish. Combing the improved CPG model [26, 27] to control the motion of robotic fish, we achieved the mission of target tracking.

The rest of this paper is organized as follows. Section 2 describes the mechatronic design of the robotic fish, including mechanical design and electronics. Section 3 presents a target tracking strategy based on multi-sensor information fusion. Section 4 shows the experimental results. Finally, Section 5 contains conclusions and future work.

II. THE SYSTEM DESIGN OF ROBOTIC FISH

The target tracking experiments are carried out on a robotic fish that has multiple swimming modes, such as cruising, turning, and pitching. This section mainly introduces the mechatronics design and motion control of the robot. The present robot is an improved version and holds the following improvements compared with the old version [26]: 1) higher scalability; 2) good watertight design; 3) easy to assemble; and 4) multiple sensors.

A. Mechatronics Design

As shown in Fig. 1, we design a fish-inspired robot platform, which consists of three parts: a rigid head, a wire-driven active body, and a compliant tail. The electronic components used by the robotic fish are contained in the two waterproof sealed compartments. One is used to install the circuit board and battery, and the other is used to install the infrared sensors and LED light. Moreover, silicone gaskets are designed for each sealed cabin for waterproof sealing. At the same time, to make the robotic fish scan the objects in front of it, three infrared sensors are arranged in a symmetrical semi-circular arc arrangement, and are respectively located at the front, left, and right positions of the head of the robotic fish. Unlike treating the head swing of fish swimming as disturbance, we utilize the head swing of fish swimming, which can better help the robotic fish to extend the detection range of the target or obstacle in front of it. The role of the robotic fish dorsal fin can not only effectively prevent rollover, but also increase the space for installing the switch. The hollow joint design can not only reduce the weight of the robotic fish, but also can be filled with buoyancy materials to adjust the overall buoyancy. The design specifications of the robotic fish are detailed in Table 1. The design of other parts (i.e. the active body and compliant tail) can be examined in our previous work [20].

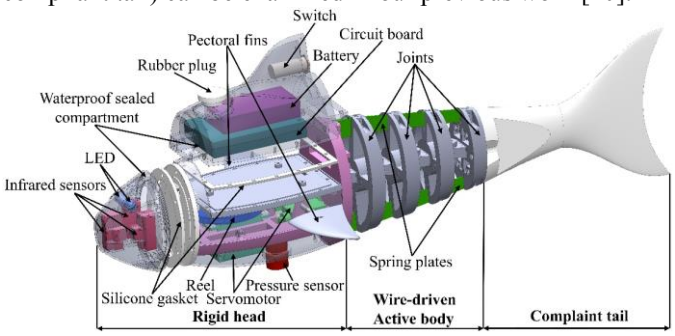

Fig. 1. The design of the fish-inspired robot platform.

TABLE I
THE DESIGN SPECIFICATIONS OF THE ROBOT FISH

Items	Specifications
Dimensions (mm^3)	492(L) × 233(W) × 157(H)
Mass (g)	1122
Microcontroller	STM32F103
Battery	7.4VDC 1500-mAH Ni-H battery
Servomotors	SAVOX SW-1210S (Active body) Hitec HS-5086WP (Pectoral fins)
Infrared sensors	GP2Y0A21
Communication module	E62-433T20D
Inertial Measurement Unit (IMU)	MPU60501
Pressure sensor demagnetizing	B30

B. Motion Control

The central pattern generator (CPG) is a neuron circuit that can produce rhythmic movement without the sensation or high-level input carrying specific timing information [28]. Similarly, fish also swim in a rhythmic movement. Therefore, we can employ the CPG model to generate rhythmic movement for the robotic fish. Our team studied Ijspeert's CPG model, which has been successfully applied to the salamander robot [29], and proposed an improved CPG model including a new parameter, time ratio R [26]. The equation of

the improved CPG model is as:

$$\ddot{b} = k_b\left(0.25k_b(B-b)-\dot{b}\right), \quad (1)$$

$$\ddot{m} = k_m(0.25k_m(M-m)-\dot{m}), \quad (2)$$

$$\dot{\phi} = \left[\frac{(1+R)^2}{4R} - \frac{R^2-1}{4R}\text{sign}(\sin\phi)\right]\omega, \quad (3)$$

$$\alpha = b + m\cos(\phi), \quad (4)$$

$$\beta = b + m\sin(\phi), \quad (5)$$

where b denotes the offset state, B indicates the high-level control command of offset, k_b is a positive constant determining how fast b converges to B; m represents the amplitude state, M indicates the high-level control command of amplitude, k_m is a positive constant determining how fast m converges to M; ϕ denotes the phase state; R is the time ratio between restore phase (t_r) and beat phase (t_b) in one period. ω denotes the high-level control command of angular velocity; α is the rotation angle of the servomotor; and β is an intermediate variable. Here, we set $k_b = 20$ and $k_m = 20$ based on testing.

This improved CPG model has four input control parameters: the amplitude M, the angular velocity ω, the offset B, and the time ratio R, respectively. The robotic fish can be controlled to cruise or turn through adjusting these four input parameters, (M, ω, B, R). For cruising, $M \neq 0$, $\omega \neq 0$, $B = 0$, and $R = 1$, while turning, $M \neq 0$, $\omega \neq 0$, $B \neq 0$, and $R > 1$.

The only output parameter α, which is used as the rotation angle of servomotor, thereby indirectly controlling the bending angle of the active body, Φ. The relationship between the angles, α, and Φ can be simplified as:

$$\Phi = \frac{2r}{d}\alpha. \quad (6)$$

where r denotes the radius of the reel, d is the distance between two wires. For the robotic fish specifications we designed, $r = 33$ mm, $d = 36$ mm. It is obvious from the simplified formula that α and Φ are proportional.

III. Control Strategy Based on Multi-sensor Information Fusion

A. Scarce Sensing Information Fusion Strategy

It is a challenge to distinguish obstacles and the target without using the camera. Here, we adopt infrared sensors as the primary sensors for the robotic fish. The output voltage value of the infrared sensor decreases with the increase of the detection target distance. As depicted in Fig. 2, the results indicate that the sensors' recognition distance range in water is approximately 10cm–60cm. According to the working characteristics of the infrared sensor, different voltage thresholds can be set according to the different distances of the objects that need to be detected. In the experiment of this paper, the threshold distance value for the infrared sensor to detect objects is set to 25cm, and the corresponding voltage threshold is 1.5V. If the distance is too close, the robotic fish may collide with the tracking target easily; and if the distance is too far, the robotic fish may lose track of the target, thus, a moderate distance value is selected. Then, through comparing the output voltage of the infrared sensor with the voltage threshold, a decision can be made. Because the infrared sensors can only measure distances but cannot identify objects, when the robotic fish performs target tracking tasks, the robotic fish may not identify if it is the tracking target, pool walls, obstacles, or other objects, causing the mission to fail. Therefore, we presented a target tracking strategy based on the scarce sensing information fusion by analyzing and combining the information of two adjacent consecutive moments of the sensors. Multi-sensor information fusion is utilized to improve the overall reliability of the detection system.

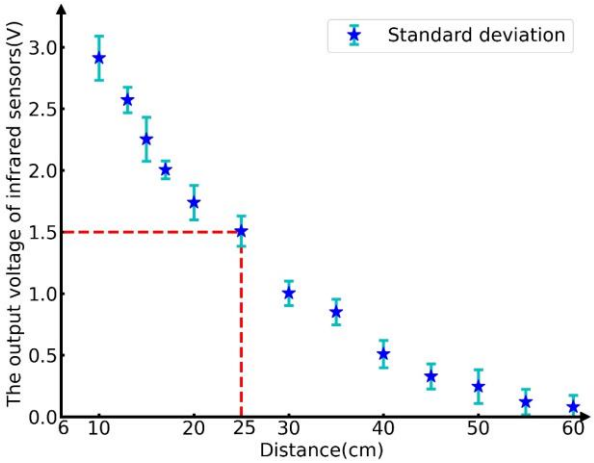

Fig. 2. The voltage output characteristics of the infrared sensors in the water.

Each infrared sensor has only 2 states at each moment, that is, whether the object is in its detection range; and the three infrared sensors have a total of 8 states. Then, there are 64 states when the signals of two consecutive moments are combined. The target tracking strategy adopted in this paper is proposed based on the following assumptions, and the priority of the assumptions is reduced: 1). The target has always been within the tracking range of the robotic fish, that is, there must be a signal for the target at a later moment. 2). If there is no signal at the later moment, the robotic fish will move according to the movement state of the previous moment. 3). If there is no signal at the previous moment, that is, when the tracking task is just started, set the target to be in front of the robotic fish. When the signal value collected by the sensor is less than 1.5V, it is judged that no object is detected, otherwise, it is detected. Table 2 shows an example of 8 states of them, in which T0 and T1 are two consecutive adjacent moments. In these 8 states, the data collected by the sensor at T0 moment are all less than 1.5V, while the T1 moment is a combination of all 8 possible states. The states 1, 2, 3 can be derived according to the first assumption. Since there is no signal at the previous moment, the robotic fish is in the starting state by default. When there are multiple signals at the next moment, the robotic fish performs the forward movement, such as the states 4, 5, 6, and 7. This complies with the third assumption. As for state 0, which is impossible to occur, the motion of the robotic fish is set forward. The various remaining 56 states can be derived according to the above three assumptions.

TABLE II

THE TARGET TRACKING STRATEGY BASED ON MULTI-SENSOR INFORMATION FUSION CENTRALIZED DETECTION

States	Input						Output
	T0			T1			
	Front	Left	Right	Front	Left	Right	
0	0.79	0.97	1.11	0.81	0.51	0.75	Forward
1	1.08	0.28	0.49	1.76	0.15	0.78	Forward
2	0.11	1.28	1.46	0.63	3.22	1.06	Turn left
3	0.25	0.51	1.43	0.54	1.32	2.09	Turn right
4	0.46	1.47	0.06	1.72	3.06	1.08	Forward
5	1.27	1.48	0.75	2.79	0.42	1.77	Forward
6	1.49	1.25	1.32	1.03	1.64	2.27	Forward
7	1.27	1.41	0.58	2.38	1.69	1.61	Forward

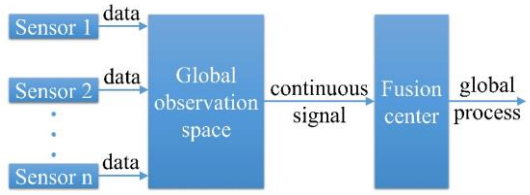

Fig. 3. Multi-sensor information fusion centralized detection.

Next, we adopt a centralized detection method to develop a target tracking strategy. The centralized detection, as shown in Fig. 3, is to directly transmit all the original information received by multiple sensors to the fusion center, which is the target tracking strategy of 64 states. Then, the fusion center processes this information globally to obtain the detection result of the target object. In the centralized detection, the signals collected by the sensors do not need to undergo separate preprocessing, and the final signal transmitted to the fusion center is the original continuous signal. Then, the corresponding 64 states can be derived based on the three assumptions mentioned above, of which 8 states are shown in Table 2.

Each of these 64 states has 6 inputs (3 for T0 and 3 for T1) and 1 output, but there are 3 types of outputs, namely forward, turn left and turn right. From the overall point of view, this tracking strategy is a three-category problem, which is to judge different input data and then generate the corresponding output. The tracking strategy of 64 states can be converted into training samples, and the model can be generated by using machine learning. Then, the data collected by the sensors is directly input into the trained model to generate the correct classification results. In this paper, the decision tree model, which is a typical machine learning method, is adopted to train and classify the tracking strategies of the centralized detection. Here, the information gain (ID3 algorithm) in the "Impurity" index, which refers to the size of uncertainty, is employed to construct the decision tree[30]. Information gain means that division can bring about an increase in purity and a decrease in information entropy. Information entropy is a measure of the uncertainty of a signal or distribution. The information entropy of perfect data segmentation is 0. The formula of information entropy and information gain is as follows:

$$Entropy(t) = -\sum_{i=0}^{c-1} p(i|t) \log_2 p(i|t), \quad (7)$$

$$Gain(D, a) = Entropy(D) - \sum_{i=1}^{k} \frac{|D_i|}{|D|} Entropy(D_i). \quad (8)$$

where $p(i|t)$ represents the probability that node t is category i, D is the parent node, D_i is the child node, and a in $Gain(D, a)$ is used as the attribute selection of the D node.

Therefore, the calculation formula for information gain is the information entropy of the parent node minus the information entropy of all child nodes. The decision tree of

Fig. 4. The decision tree of centralized detection.

centralized detection constructed by information gain is shown in Fig. 4. It can be observed that when the information entropy is 0, the classification is successful. The brown, green, and purple tree nodes are the results of successful classification, representing forward, turn left, and turn right, respectively. The results show that the centralized detection decision tree has few branches, fast convergence, and high purity.

Based on the tracking strategy, the target tracking control structure diagram of the robotic fish is shown in Fig. 5. The corresponding target tracking strategy is set according to the setting of different input voltage thresholds. Then, the data collected by the infrared sensor on the robotic fish generates continuous signals through centralized detection and is input to the trained decision tree model, which will generate the input parameters of the CPG model. The default CPG model parameters are $(M, \omega, B, R) = (20, 4\pi, 0, 1)$ for cruising straightly, and default parameters $(M, \omega, B, R) = (30, 4\pi, \pm 30, 2)$ for steering a turn for the robotic fish. The CPG model finally outputs the rotation angle α of the servomotor to control the movement of the robotic fish.

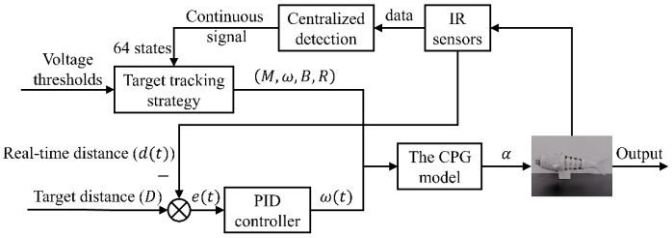

Fig. 5. The target tracking control structure of the robotic fish.

B. PID Closed-Loop Control for Adjustable Speed

The PID closed-loop control is mainly used for robotic fish to adjust its swimming speed in real-time according to the distance between itself and the tracking target. In Fig. 5, the input signal of PID closed-loop control is the target distance (D), and the feedback signal is the real-time distance $d(t)$ between the robotic fish and the tracking target. Since the sampling frequency of the infrared sensor is too high (100 Hz) compare to the motion cycle of robotic fish, if every real-time collected information is processed, the robotic fish will not have time to respond accordingly in one motion cycle. Eventually, the motion speed will not be converted smoothly, and the motion will be stuck. To deal with this situation, we collect 10 signals each time for averaging processing and then feed them back into the PID controller. Thus, the real-time distance $d(t)$ between the robotic fish and the tracking target can be calculated as:

$$d(t) = \frac{1}{N}\sum_{i=1}^{N} d_i(t), \tag{9}$$

where $N(N = 10)$ is the number of times the signal is sampled, and $d_i(t)(i = 1, 2, \ldots, 10)$ is the real-time distance of the ith sampling at the same time interval.

The deviation signal $(e(t))$, which is the input of PID controller, is calculated as:

$$e(t) = D - d(t), \tag{10}$$

The flapping angular velocity $\omega(t)$, one of the CPG model input parameters, can be obtained through PID controller, and the equation is as follows:

$$\omega(t) = K_p \times e(t) + K_i \times \int_0^t e(\tau)d\tau + K_d \times \frac{de(t)}{dt}, \tag{11}$$

$$\omega(t) = \begin{cases} 4\pi, & \omega(t) \le 0 \\ 4\pi - \omega(t) \times \frac{(45-0)}{2\pi}, & 0 < \omega(t) < 45. \\ 2\pi, & \omega(t) \ge 45 \end{cases} \tag{12}$$

where $\omega(t)$ is the only variable CPG parameter to adjust the swimming speed of the robotic fish, and K_p, K_i and K_d denote the proportional, integral, and derivative coefficients of the PID controller, respectively. Before the experiment, we first test the speed changes of the robotic fish at different distances between itself and the tracking target and determined the values of K_p, K_i and K_d to be 3, 0, and 0.05, respectively. Finally, a piecewise function is used to determine the output signal $\omega(t)$ of the PID controller so that the robotic fish can adjust its speed in real-time. The value of $\omega(t)$ generated by the PID will override the $\omega(t)$ value output by the decision tree to adjust the speed without affecting the motion decision.

IV. Experiments

To validate the target tracking strategy of the robotic fish, several sets of experiments are conducted in a pool with the dimensions of 4000m×2110mm×1000mm. The experimental platform is shown in Fig. 6. A camera is installed on a frame that is 3m above the ground and is used to record the experimental process. There is a hand-held moving arc-shaped baffle acting as the tracking target of the robotic fish to assist in completing the experiment. Due to the sweep range limitation of the infrared sensor, we chose the arc-shaped baffle as the target to ensure that the robotic fish would detect at least one signal at any time.

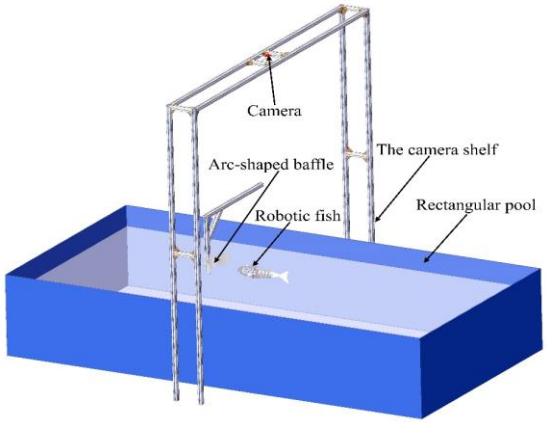

Fig. 6. The experimental platform of the robotic fish.

A. Simulation

Before carrying out the experiments, it is necessary to verify the validity of the target tracking strategy via simulation. The simulation is realized through python and imitates the working condition of the real infrared sensors, when infrared sensors recognize the target, pool wall, or obstacle, they will enter the sensing state. The two signals at adjacent consecutive moments will be recorded and input into the tracking strategy of 64 states to obtain the corresponding output. Then, different tracking target trajectories will be set through simulation to

check whether the sensor can actually work and complete the target tracking tasks. Fig. 7 (a) and (b) depict the simulation results of the robotic fish target tracking along the curved trajectory, and tracking the target with an obstacle disturbance, respectively. As shown in Fig. 7 (a), the robotic fish can complete tracking the curved trajectory, while the result is not very satisfying since the robotic fish is only set to swim straightly to track the target. As shown in Fig. 7(b), the robotic fish can track the target while avoiding the obstacle disturbance. Since the simulation does not consider the head swinging and the turning radius of the robotic fish, the trajectory of the simulation result does not fluctuate and the angle of 90° can be turned by only one turning movement. Although this simulation experiment was carried out under ideal conditions, the simulation results can verify the feasibility of the target tracking strategy proposed in this paper. Next, it will be further verified through actual experiments.

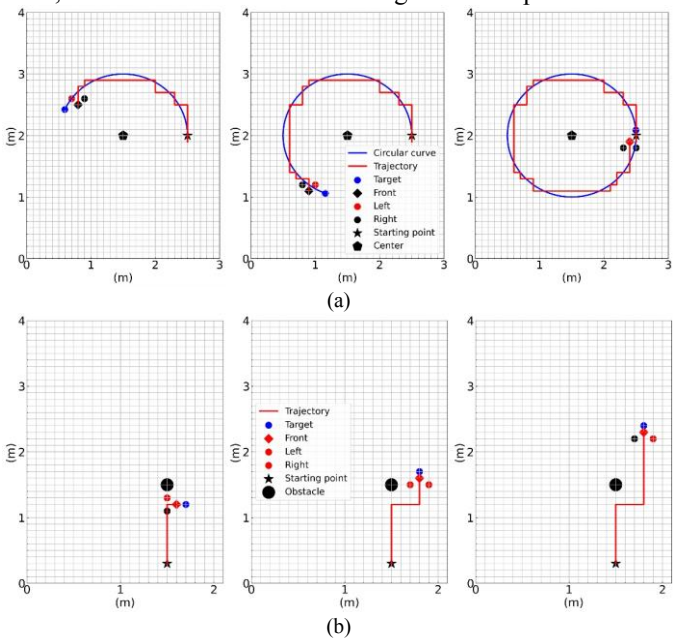

Fig. 7. The simulation results of the (a) target tracking along curved trajectories, (b) target tracking with an obstacle disturbance. (The solid blue line represents the circular curve of the tracking target. The solid red line represents the motion trajectory of the robotic fish. The blue dot represents the tracking target. The black diamond and two black dots represent the infrared sensors on the front, left, and right of the robotic fish, respectively. When the infrared sensors recognize an object, the black diamond and dots will change from black to red. The black star represents the starting position of the tracking process. The black pentagon is the mark point of the center of the circle. The larger black dot is the obstacle.)

B. Target Tracking Along Straight Line

The target tracking along straight-line experiment is mainly to verify whether the robotic fish could adjust its swimming speed according to the distance from the front target. The robotic fish adopts the PID closed-loop feedback control as mentioned above to change the flapping frequency in real-time to adjust its swimming speed. In this experiment, we set a fixed distance value of 25 cm between the robotic fish and the tracking target. Because the robotic fish swims along the straight line in this experiment, only one set of CPG control parameters needed to be set. The three CPG parameters M, B, and R are set as constant, which are 20, 0, and 1, respectively. The other parameter ω is continuously updated by the PID controller. The coefficients K_p, K_i, and K_d of the PID controller are 3, 0, and 0.05, respectively, which are obtained from the analysis in Section 3.

Fig. 8 shows the results of target tracking along straight-line experiment, and the real-time output value α of the CPG model and the distance to the tracking target of the robotic fish can be seen in Fig. 9. During the period of 0s to 4.16s, the tracking target is rather far away from the robotic fish, to catch up with the target, the robotic fish increases the flapping frequency to swims fast. The same scenario occurred after 8.22s. At 4.16s, the robotic fish began to approach the tracking target. To prevent the robotic fish from hitting the tracking target, the robotic fish reduced its flapping frequency to slow down. The results fully demonstrate the feasibility and effectiveness of the PID closed-loop control.

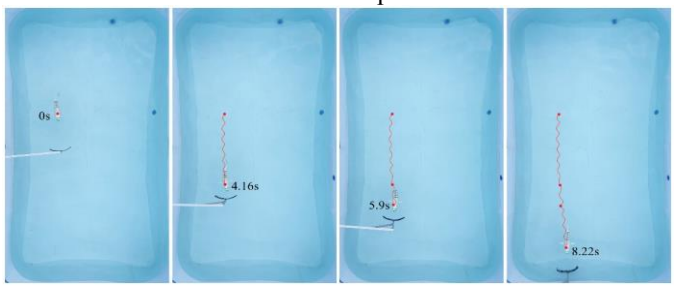

Fig. 8. The target tracking along straight line experiment of the robotic fish.

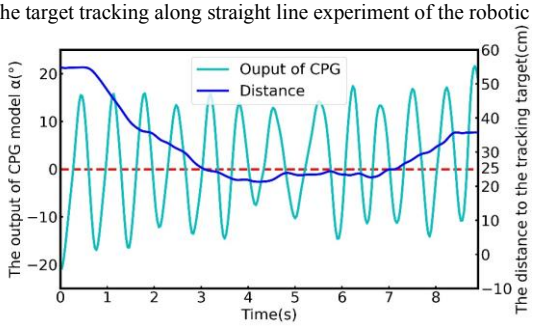

Fig. 9. The output value α of the CPG model and the distance to the tracking target of the robotic fish.

C. Target Tracking Along Curved Trajectories

The robotic fish not only can achieve straight-line tracking, but also track the target in a curved manner. In this experiment, we conduct an S-shaped trajectory tracking. The CPG parameter settings are the same as mentioned above, when the robotic fish cruises straight; whereas M, ω, B, and R are 30, 4π, ± 30, and 2, respectively, when the robotic fish makes a turn.

As shown in Fig. 10, the robotic fish can track the S-shaped trajectory of the target (manual moved) in around 9s. Fig. 11 shows the real-time output value α of the CPG model, which is the control parameter of the robotic fish in the S-shaped trajectory experiment. The different colored blocks in the figure represent the different motions of the robotic fish (i.e. cruise, turn left, and turn right). From 0s to 1.9s, the robotic fish mainly cruises in a straight line, and it also performs a left turn to adjust its direction. After 1.9s, the robotic fish again adjusted its direction by turning right, and then the robotic fish cruised straight to 5.08s. Subsequently, the robotic fish keeps

turning left and finally forms a complete S-shaped curved trajectory. From the experiment, it can be expected that the robotic fish can track complex curved trajectories.

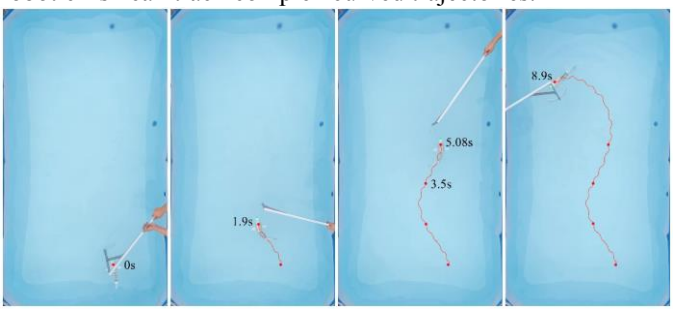

Fig. 10. The S-shaped curved trajectory tracking experiments of robotic fish.

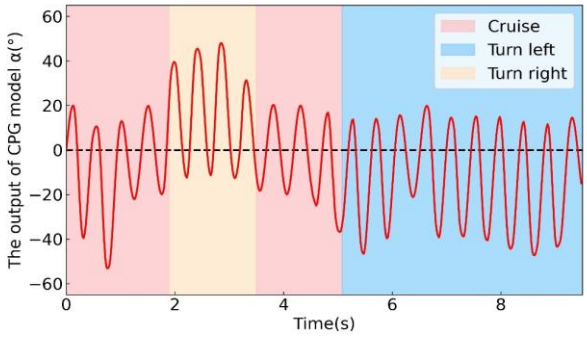

Fig. 11. The output value α of the CPG model of the robotic fish in the S-shaped curved trajectory tracking experiment.

D. Target Tracking with An Obstacle Disturbance

In practical situations, we consider that obstacles may appear on the swimming route of the robotic fish during the tracking task. Therefore, it is necessary to carry out corresponding target tracking experiments in this scenario. At the beginning, we placed an obstacle about 1.5m in front of the robotic fish, as shown in Fig. 12. At 1.4s, we started to move the target to guide the robotic fish to move. At this time, the infrared sensor on the right side of the robotic fish detected the target and turned right. Then, at 2.3s, the left sensor detected the presence of an obstacle, and it can still make a correct decision to move forward for tracking the target. Then, when the robotic fish is about to hit the wall of the pool, the right sensor can detect the pool wall, but the robotic fish can still distinguish which is the tracking target, and turn left to avoid hitting the wall and track the target to the end.

Fig. 13 (a) shows the real-time infrared sensors signals in the experiment, where the threshold value set for the three infrared sensors is 1.5V; and the CPG model output of the robotic fish at the corresponding time and the state of motion of the robotic fish in each time period are shown in Fig. 13 (b). The darker color blocks in Fig. 13 (a) are the raw data collected by the three infrared sensors, and the lighter color blocks are the motion judgments generated by the robotic fish through the tracking strategy based on the sensor information. The motion states of the robotic fish in the two subgraphs in Fig. 13 are consistent. Fig. 14 shows the confusion matrix of the training set and test set of the decision tree model respectively. From the confusion matrix of the training set, it can be seen that the predicted result of the decision tree model is completed correctly, and there is no overfitting. Then we randomly select 32 sets of infrared sensor data at consecutive moments as the test set through 10 times and input the test set into the trained decision tree, and finally, an average accuracy of 96.875% can be obtained. The result shows that the target tracking strategy is feasible and effective. What's more, the success of this experiment proves that the target tracking strategy is suitable for robotic fish to track targets in a variety of situations.

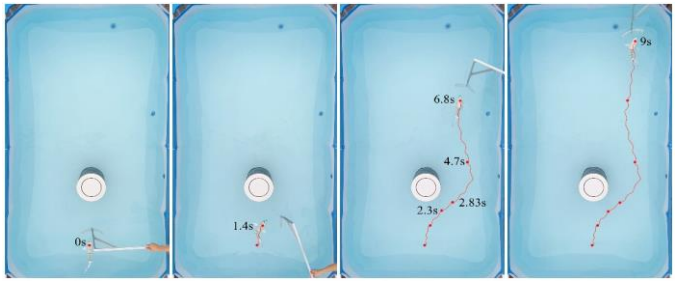

Fig. 12. The target tracking with an obstacle disturbance.

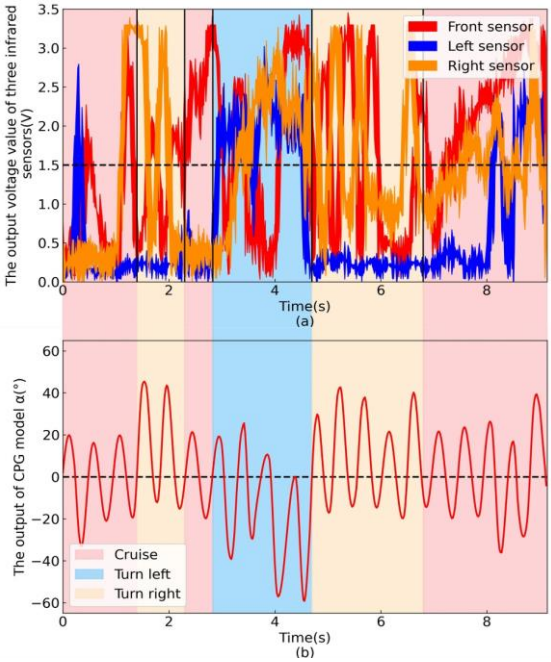

Fig. 13. (a) The output voltage value of the front, left, and right infrared sensor; (b) The output value α of the CPG model of the robotic fish in the target tracking experiment with an obstacle disturbance.

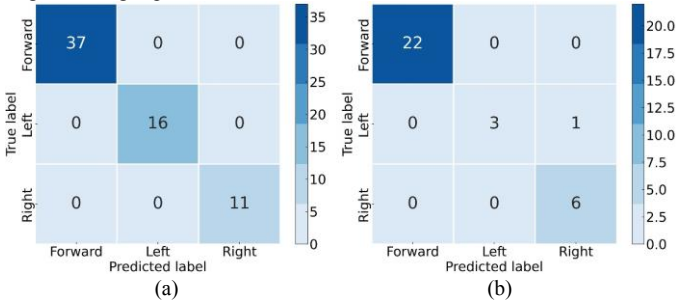

Fig. 14. The confusion matrix of the decision tree model of the (a) training set and (b) test set.

V. Discussions and Conclusions

In this paper, we investigated the possibility of utilizing sensors that could only detect the appearance of objects within the sensing range to achieve target tracking of the robotic fish.

The infrared sensors adopted in this work are just one option, which can be replaced by sensors of similar functions, such as ultrasonic transducers, and laser sensors. Normally, the scarce sensing information of infrared sensors is hard to execute underwater target-tracking tasks. However, through our target tracking strategy, which fuses the sensing information, and analyzes and combines the information of two adjacent consecutive moments of the sensors, we can achieve target tracking with obstacles disturbances. The strategy is trained and classified through the decision tree based on centralized detection. Through Simulations and experiments, the following conclusions can be obtained: 1) The robotic fish can adjust its speed in real-time according to the distance to the tracking target; 2) The robotic fish can achieve target tracking of complex trajectories; 3) Even in the presence of obstacles and pool wall, the robotic fish can accurately track the target. The results prove the feasibility and effectiveness of the target tracking strategy, and also show the possibility of utilizing low-cost scarce sensing information for underwater target tracking even without a camera. Moreover, in real applications, sensors with a longer detection range can also be selected, but the size of the robotic fish needs to be redesigned accordingly.

However, we know that such type of sensors has many limitations, one cannot execute underwater tracking tasks relying on this type of sensors alone. We believe the idea in this paper will offer valuable insight about dealing with low-quality and scarce underwater sensing information for underwater robots to execute tasks, and at least can be an auxiliary approach for underwater tracking systems with multiple types of sensors.

References

[1] M. S. Triantafyllou and G. S. Triantafyllou, "An Efficient Swimming Machine," *Scientific American,* vol. 272, pp. 64-70, 1995.

[2] R. Du, Z. Li, Y. Kamal, and V. Pablo, "Robot fish," *Berlin, Heidelberg: Springer,* vol. 10, pp. 978-3, 2015.

[3] J. Liu, H. Hu, and D. Gu, "A Hybrid Control Architecture for Autonomous Robotic Fish," in *2006 IEEE/RSJ International Conference on Intelligent Robots and Systems*, 2007.

[4] C. Zhou and K. H. Low, "Design and Locomotion Control of a Biomimetic Underwater Vehicle With Fin Propulsion," *IEEE/ASME Transactions on Mechatronics,* vol. 17, pp. 25-35, 2012.

[5] P. Kodati, J. Hinkle, A. Winn, and X. Deng, "Microautonomous Robotic Ostraciiform (MARCO): Hydrodynamics, Design, and Fabrication," *IEEE Transactions on Robotics,* vol. 24, pp. 105-117, 2008.

[6] W. Wang and G. Xie, "Online High-Precision Probabilistic Localization of Robotic Fish Using Visual and Inertial Cues," *IEEE Transactions on Industrial Electronics,* vol. 62, pp. 1113-1124, 2015.

[7] J. Yu, R. Ding, Q. Yang, M. Tan, W. Wang, and J. Zhang, "On a Bio-inspired Amphibious Robot Capable of Multimodal Motion," *IEEE/ASME Transactions on Mechatronics,* vol. 17, pp. 847-856, 2012.

[8] R. K. Katzschmann, J. Delpreto, R. Maccurdy, and D. Rus, "Exploration of underwater life with an acoustically controlled soft robotic fish," *Science Robotics,* vol. 3, p. eaar3449, 2018.

[9] Y. Zhong, J. Song, H. Yu, and R. Du, "A study on kinematic pattern of fish undulatory locomotion using a robot fish," *Journal of Mechanisms and Robotics,* vol. 10, p. 041013, 2018.

[10] Y. Zhong, J. Song, H. Yu, and R. Du, "Toward a Transform Method From Lighthill Fish Swimming Model to Biomimetic Robot Fish," *IEEE Robotics and Automation Letters,* vol. 3, pp. 2632-2639, 2018.

[11] Y. Zhong, Z. Li, and R. Du, "A Novel Robot Fish With Wire-Driven Active Body and Compliant Tail," *IEEE/ASME Transactions on Mechatronics,* vol. 22, pp. 1633-1643, 2017.

[12] Y. Hu, W. Zhao, G. Xie, and L. Wang, "Development and target following of vision-based autonomous robotic fish," *Robotica,* vol. 27, pp. 1075-1089, 2009.

[13] Y. Hu, Z. Wei, and L. J. I. T. o. I. E. Wang, "Vision-Based Target Tracking and Collision Avoidance for Two Autonomous Robotic Fish," vol. 56, pp. 1401-1410, 2009.

[14] G. Ferri, A. Munafo, and K. D. J. I. J. o. O. E. LePage, "An autonomous underwater vehicle data-driven control strategy for target tracking," vol. 43, pp. 323-343, 2018.

[15] F. Mandić, I. Rendulić, N. Mišković, and Đ. J. J. o. S. Nađ, "Underwater object tracking using sonar and USBL measurements," vol. 2016, 2016.

[16] D. Shin, S. Y. Na, J. Y. Kim, and S.-J. Baek, "Fish Robots for Water Pollution Monitoring Using Ubiquitous Sensor Networks with Sonar Localization," presented at the 2007 International Conference on Convergence Information Technology (ICCIT 2007), 2007.

[17] M. Ji, Z. Yong, X. Zheng, G. Liu, and Q. Jing, "A fish-shaped minimal prototype of lateral line system based on pressure sensing," in *2017 IEEE International Conference on Mechatronics and Automation (ICMA)*, 2017.

[18] W. Wang, D. Gu, and G. Xie, "Autonomous Optimization of Swimming Gait in a Fish Robot With Multiple Onboard Sensors," *IEEE Transactions on Systems, Man, and Cybernetics: Systems,* vol. 49, pp. 891-903, 2019.

[19] X. Zheng, W. Wang, L. Li, and G. Xie, "Artificial lateral line based relative state estimation between an upstream oscillating fin and a downstream robotic fish," *Bioinspir Biomim,* Sep 14 2020.

[20] J. Chen, B. Yin, C. Wang, F. Xie, R. Du, and Y. Zhong, "Bioinspired Closed-loop CPG-based Control of a Robot Fish for Obstacle Avoidance and Direction Tracking," *Journal of Bionic Engineering,* vol. 18, pp. 171-183, 2021.

[21] Y. Hu, W. Zhao, L. Wang, and Y. Jia, *Underwater target following with a vision-based autonomous robotic fish*, 2009.

[22] J. Yu, W. Kai, T. Min, and J. Zhang, "Design and Control of an Embedded Vision Guided Robotic Fish with Multiple Control Surfaces," *Scientific World Journal,* vol. 2014, p. 631296, 2014.

[23] J. Yu, F. Sun, D. Xu, and M. Tan, "Embedded Vision-Guided 3-D Tracking Control for Robotic Fish," *IEEE Transactions on Industrial Electronics,* vol. 63, pp. 355-363, 2016.

[24] J. Shao, L. Wang, and J. Yu, "Development of multiple robotic fish cooperation platform," *International Journal of Systems Science,* vol. 38, pp. 257 - 268, 2007.

[25] J. Yu, T. Min, and L. Wang, *Cooperative Control of Multiple Biomimetic Robotic Fish*: Recent Advances in Multi Robot Systems, 2008.

[26] F. Xie, Y. Zhong, R. Du, and Z. Li, "Central Pattern Generator (CPG) Control of a Biomimetic Robot Fish for Multimodal Swimming," *Journal of Bionic Engineering,* vol. 16, pp. 222-234, 2019.

[27] F. Xie, Z. Li, Y. Ding, Y. Zhong, and R. Du, "An Experimental Study on the Fish Body Flapping Patterns by Using a Biomimetic Robot Fish," *IEEE Robotics and Automation Letters,* vol. 5, pp. 64-71, 2020.

[28] A. J. Ijspeert, "Central pattern generators for locomotion control in animals and robots: a review," *Neural Netw,* vol. 21, pp. 642-53, May 2008.

[29] Ijspeert, A. Jan, Crespi, Alessandro, Ryczko, Dimitri, *et al.*, "From Swimming to Walking with a Salamander Robot Driven by a Spinal Cord Model," *Science,* 2007.

[30] H. Han, M. Feng, and W. Y. Wang, "Review of Recent Development in Decision Tree Algorithm in Data Mining," *Application Research of Computers,* 2004.